

Ion Adsorption at the Rutile-Water Interface: Linking Molecular and Macroscopic Properties

Z. Zhang,^{1,2} P. Fenter,¹ L. Cheng,¹ N.C. Sturchio,^{1,3} M.J. Bedzyk,^{1,2} M. Předota,^{4,5}
P.T. Cummings,⁵ M.L. Machesky,⁶ D.J. Wesolowski⁷

¹Argonne National Laboratory, Argonne, IL, U.S.A.

²Institute of Environmental Catalysis (IEC), Northwestern University (NU), Evanston, IL, U.S.A.

³University of Illinois at Chicago, IL, U.S.A.

⁴Institute of Chemical Process Fundamentals, Prague, Czech Republic

⁵Vanderbilt University, Nashville, TN, U.S.A.

⁶Illinois Water Survey, Champaign, IL, U.S.A.

⁷Oak Ridge National Laboratory, Oak Ridge, TN, U.S.A.

Introduction

Electrical double layers (EDLs), which form spontaneously at oxide-water interfaces by adsorption or desorption of ions [1], influence many natural and industrial processes [2]. Classical diffuse-condensed layer models of EDLs and their modern successors that incorporate discrete ion binding sites — collectively known as surface complexation models (SCMs) — have proven to incorporate some of the most useful and successful theories of complex fluid-solid interfaces. They provide a broad framework from which to conceptualize EDL properties and quantify the macroscopic effects of charge separation. However, the ability of these conceptual models to incorporate molecular-scale information has yet to be firmly established, and structural parameters derived from such models are ambiguous.

Prior to the current study, the exact termination and structure of a rutile surface in contact with dense liquid water had not been determined experimentally, and little was known about the specific locations of ions adsorbed to this surface, with a few exceptions [3-5]. In this study, we combine *in situ* synchrotron x-ray measurements on submerged rutile (110) single-crystal surfaces with *ab initio* calculations, molecular-dynamic (MD) simulations, and macroscopic data from bulk titrations and electrophoresis studies of rutile powders to obtain an integrated understanding of the EDL that connects the actual molecular structures to the macroscopic properties [6].

Methods and Materials

Crystal truncation rod (CTR) measurements [7] of the rutile-aqueous interface structure were performed with the rutile crystal in contact with deionized water and $[\text{Rb}^+] = 1 \text{ mol/kg}$, $\text{pH} = 12$ solutions, respectively. X-ray standing wave (XSW) data with the (110), (111), (200), (101), and (211) reflections were measured. Solution conditions for the XSW triangulation measurements were $10.49 \text{ } \mu\text{mol/kg ZnTr}_2$ at $\text{pH} = 8.0$, $104.4 \text{ } \mu\text{mol/kg SrCl}_2$ at

$\text{pH} = 10.7$, and $11.2 \text{ } \mu\text{mol/kg Y}(\text{NO}_3)_3$ at $\text{pH} = 6.11$. Details of surface titration measurements, the molecular dynamic, and *ab initio* calculations can be found in reference [6].

Results

Representative specular and nonspecular x-ray reflectivity (XR) for rutile (110) in contact with pure water are shown in Fig. 1(B). In addition to the (2,0) and (0,2) CTRs that are shown, the (0,0) and (1,1) CTRs were also measured. The best-fit model was then converted to a laterally averaged electron density profile (incorporating the finite resolution of the experimental data), as shown in Fig. 1(C). These data reveal that the crystal is terminated by rows of bridging oxygen (BO) sites and terminal oxygen (TO) sites lying $1.17 \pm 0.02 \text{ } \text{Å}$ and $2.12 \pm 0.02 \text{ } \text{Å}$, respectively, above the surface plane. An additional layer of adsorbed water molecules, $\sim 3.8 \text{ } \text{Å}$ above the surface plane [Fig. 2(C)], is found in laterally ordered sites characterized as bridging between the surface oxygen sites. [Note, however, that derived oxygen atom locations from these XR data are degenerate to translations of $(a/2)\mathbf{i} + (b/2)\mathbf{j}$ (where $a = 6.50 \text{ } \text{Å}$ and $b = 2.96 \text{ } \text{Å}$ are the surface unit cell dimensions along unit vectors \mathbf{i} [-110] and \mathbf{j} [001], respectively), since only a subset of the surface rods, having surface Miller indices $h + k = \text{even}$, were measured.] Significantly, no evidence for ordered water is observed beyond this first hydration layer.

Precise locations of Zn^{2+} , Sr^{2+} , and Y^{3+} were determined by XSW triangulation [8, 9], and the starting point for optimization using structures was obtained separately by using XSW imaging [3]. In the best-fit structure, the Sr^{2+} ions were observed to be displaced laterally by $\Delta x = \pm 0.34 \text{ } \text{Å}$ and $\Delta y = \pm 0.36 \text{ } \text{Å}$ (where x is along [-110] and y is along [001]) from the ideal tetradentate site (the site laterally equidistant to two BO and two TO sites). Y^{3+} was found in a position similar to that derived for Sr^{2+} . The heights of these two ions above the surface plane were $3.07 \pm 0.07 \text{ } \text{Å}$ (Sr^{2+}) and 2.75

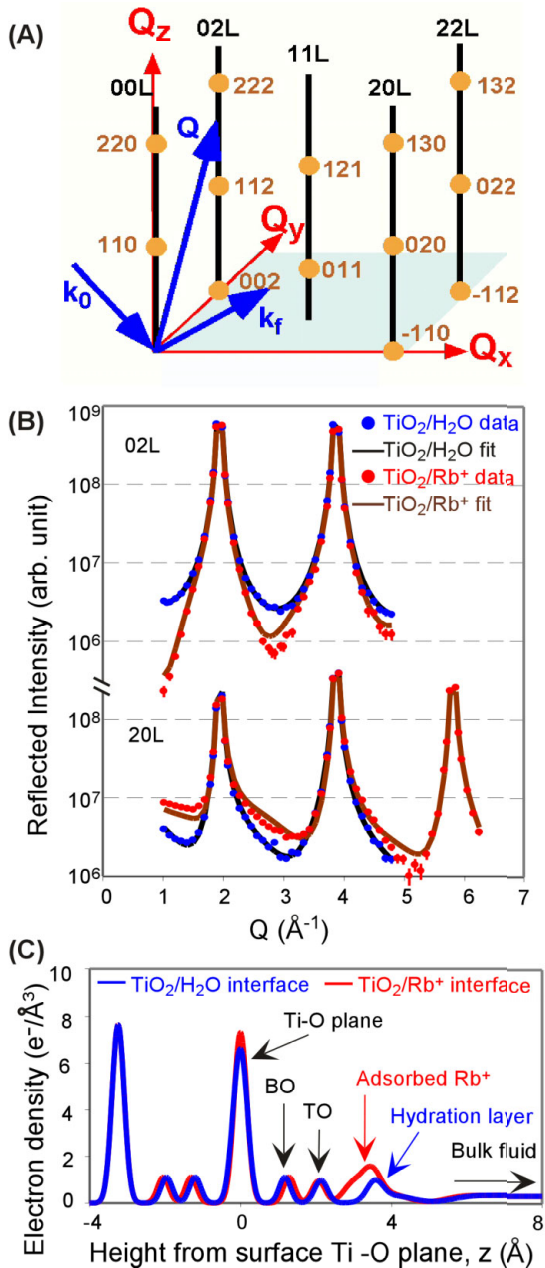


FIG. 1. (A) Reciprocal space structure of the rutile (110) surface with CTRs and bulk Bragg reflections (labeled, with surface Miller indices and bulk Miller indices, respectively). (B) Representative XRR results show the (2,0,L) and (0,2,L) CTRs for rutile in deionized water (blue circles) and $[RbCl] = 1 \text{ mol/kg}$ at pH 12 (red circles), with changes associated with Rb^+ adsorption. Lines are calculations corresponding to the best-fit structures, whose laterally averaged density profile is shown in (C).

$\pm 0.07 \text{ \AA}$ (Y^{3+}). Unlike Sr^{2+} , there was little lateral displacement of Y^{3+} away from the ideal tetradentate site (with a net displacement of $\Delta x = -0.15 \pm 0.16 \text{ \AA}$), although the direction and magnitude of this small displacement was consistent with the expectation of a single Y-O bond length to the BOs and TOs.

Zn^{2+} ions were found dominantly ($\sim 75\%$) to be above the BO at $3.12 \pm 0.06 \text{ \AA}$ from the Ti-O surface plane (with the lateral offset from the BO position, $\Delta x = 0.71 \pm 0.06 \text{ \AA}$, $\Delta y = 0.00 \pm 0.21 \text{ \AA}$). A second minor species was observed between the TO sites at $2.60 \pm 0.06 \text{ \AA}$ above the surface plane (with the lateral offset from the high-symmetry site of $\Delta x = 0.39 \pm 0.45 \text{ \AA}$, $\Delta y = 0.00 \pm 0.36 \text{ \AA}$). These results are similar to sorption sites proposed for Co^{2+} on rutile (110) from grazing-incidence extended x-ray absorption fine structure (EXAFS) measurements [4], but they provide greater insight into both the exact location of the sites and the distribution between the two sites that cannot be distinguished by EXAFS measurements.

XR measurements [Fig. 1(B)] at a pH of 12 with Rb^+ at 1 mol/kg revealed that Rb^+ also specifically adsorbs, as indicated by the significant change in the shape of the CTR. The best-fit model indicates that Rb^+ adsorbs within the surface hydration layer at a height of $3.44 \pm 0.03 \text{ \AA}$, as evidenced by the increase in electron density. Further measurements are in progress to determine the uniqueness of the lateral Rb^+ positions as well as the exact location of ordered interfacial water molecules.

Ion and interfacial water locations, derived by XR and XSW, are summarized in Fig. 2, plotted side by side with the results from the molecular dynamics simulations. These results provide reasonable adsorbed metal-surface oxygen distances, consistent with the known differences in crystallographic radii for these ions. They are also representative of the interfacial ion locations at rutile (110) in neutral to alkaline aqueous solutions over a broad range of solution conditions.

These molecular-scale insights have also been integrated into SCMs that describe proton release and cation adsorption of rutile powders that predominantly express the (110) crystal face [10]. With the relaxed surface metal-oxygen bond lengths from the *ab initio* calculations, the Multi-Site Complexation (MUSIC) model [11, 12] predicts $pH_{ppzc} = 4.8$ for rutile (110), in reasonable agreement with the powder titration results ($pH_{ppzc} = 5.4$).

The MD and x-ray observations that cation heights are insensitive to ionic strength validate Stern-based SCMs over diffuse-layer-only models. These heights, derived through a combination of experimental and computational

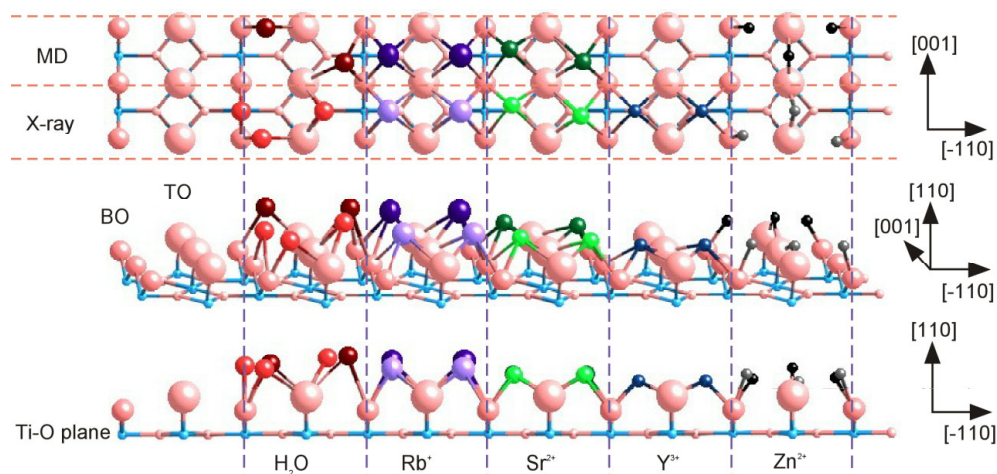


FIG. 2. (A) Top, (B) perspective, and (C) side views of the bare rutile (110) surface with BO and TO rows, and the locations of derived surface hydration and ion adsorption sites, including interfacial water, Rb^+ , Sr^{2+} , Y^{3+} , and Zn^{2+} . X-ray and MD-derived adatom locations are shaded differently, as noted in the top view. Note the close similarity of ion locations between the x-ray derived and MD-derived ion sites.

approaches, indicate that all cations are bound as inner-sphere complexes on the rutile (110) surface. This finding is consistent with the hypothesis [13] that oxides with high bulk dielectric constants are able to “hydrate” sorbed cations at least as effectively as do solvent molecules. Na^+ and Rb^+ , which are prototypical “indifferent” electrolyte cations, therefore compete directly with Ca^{2+} , Sr^{2+} , and Y^{3+} for adsorption at the tetradentate sites. Thus, the ionic-strength-dependent uptake of Ca^{2+} and Sr^{2+} on rutile is a consequence of relatively weak intrinsic binding (with respect to other divalent ions such as Zn^{2+}) coupled with competition with the more abundant background electrolyte cations.

Discussion

In summary, these XR and XSW results establish (1) the termination of the rutile surface with both terminal and bridging oxygen atoms above the Ti-O surface plane; (2) the presence of an interfacial water layer with water molecules that are both vertically and laterally ordered with respect to the rutile surface; and (3) the precise adsorption sites of various ions, including Rb^+ , Sr^{2+} , Zn^{2+} , and Y^{3+} , showing that all cations adsorb near the tetradentate site except for Zn^{2+} , which adsorbs primarily above the BO but also has a minor contribution that adsorbs between TO sites.

Acknowledgments

This work was performed at BESSRC beamline stations 12-ID-D, 11-ID-D, and 12-BM-B and XOR beamline station 1-BM-C at the APS and at beamline

X15A at the National Synchrotron Light Source. The work at these beamlines and use of the APS are supported by the U.S. Department of Energy (DOE), Office of Science, Office of Basic Energy Sciences (BES), under Contract No. W-31-109-ENG-38. The authors thank the DOE BES Division of Chemical Sciences, Geosciences, and Biosciences for supporting this research for the project “Nanoscale Complexity at the Oxide-Water Interface.” The IEC at NU is supported by the National Science Foundation (NSF) and DOE. M. Předota acknowledges support from the grant agency of the Czech Republic (Grant No. 203/03/P083). This report was extracted from Ref. 6.

References

- [1] J. Lyklema, *Fundamentals of Interface and Colloid Science*, Vol. II (Academic Press, New York, NY, 1995).
- [2] G.E. Brown, Jr., et al, *Chem. Rev.* **99**, 77 (1999).
- [3] Z. Zhang, P. Fenter, L. Cheng, N.C. Sturchio, M.J. Bedzyk, M. Machesky, and D.J. Wesolowski, *Surf. Sci. Lett.* (in press, 2003).
- [4] S.N. Towle, G.E. Brown, Jr., and G.A. Parks, *J. Colloid Interface Sci.* **217**, 299 (1999).
- [5] P. Fenter et al., *J. Colloid Interface Sci.* **225**, 154-165 (2000).
- [6] Z. Zhang, P. Fenter, L. Cheng, N.C. Sturchio, M.J. Bedzyk, M. Předota, A. Bandura, J. Kubicki, S.N. Lvov, P.T. Cummings, A.A. Chialvo, M.K. Ridley, P. Bénézech, L. Anovitz, D.A. Palmer, M.L. Machesky, D.J. Wesolowski, *Langmuir* (submitted, 2003).

[7] For a review of XR applied to the mineral-water interface, see P. Fenter, in *Applications of Synchrotron Radiation in Low-Temperature Geochemistry and Environmental Science*, edited by P.A. Fenter, M.L. Rivers, N.C. Sturchio, and S.R. Sutton (Geochemical Society, St. Louis, MO, 2002), pp. 149-220.

[8] For a review of XSW, see M.J. Bedzyk and L. Cheng, in *Applications of Synchrotron Radiation in Low-Temperature Geochemistry and Environmental Science*, edited by P.A. Fenter, M.L. Rivers, N.C. Sturchio, and S.R. Sutton (Geochemical Society, St. Louis, MO, 2002), pp. 221-266.

[9] J.A. Golovchenko, J.R. Patel, D.R. Kaplan, P.L. Cowan, and M.J. Bedzyk. *Phys. Rev. Lett.* **49**, 560-563 (1982).

[10] M.K. Ridley, M.L. Machesky, D.A. Palmer, and D.J. Wesolowski, *Colloids Surf., A* **204**, 295 (2002).

[11] M.L. Machesky, D.J. Wesolowski, D.A. Palmer, and M.K. Ridley, *J. Colloid Interface Sci.* **239**, 314 (2001).

[12] T. Hiemstra and W.H. van Riemsdijk, *J. Colloid Interface Sci.* **179**, 488 (1996).

[13] D.A. Sverjensky, *Geochim. Cosmochim. Acta* **65**, 3643 (2001).